JACC: CARDIOVASCULAR IMAGING
VOL. 3, NO. 2, 2010

ISSN 1936-878X/10/$36.00
PUBLISHED BY ELSEVIER INC.
DOI:10.1016/j.jcmg.2009.09.025

ORIGINAL RESEARCH

Assessment of Myocardial Viability at Dobutamine Echocardiography by Deformation Analysis Using Tissue Velocity and Speckle-Tracking

Manish Bansal, MD, Leanne Jeffriess, BS, Rodel Leano, BS, Julie Mundy, MBBS, Thomas H. Marwick, MBBS, PhD

Brisbane, Queensland, Australia

OBJECTIVES Comparison of myocardial tissue-velocity imaging (TVI) and speckle-tracking echocardiography (STE) for prediction of viability at dobutamine echocardiography (DbE).

BACKGROUND Use of TVI-based strain imaging during DbE may facilitate the prediction of myocardial viability but has technical limitations. STE overcomes these but requires evaluation for prediction of viability.

METHODS We studied 55 patients with ischemic heart disease and left ventricular systolic dysfunction (left ventricular ejection fraction <0.45) who were undergoing DbE for assessment of myocardial viability and who subsequently underwent myocardial revascularization. TVI was used to measure longitudinal end-systolic strain (longS) and peak systolic strain rate (SR) at rest and at low-dose dobutamine (LDD). Longitudinal, radial, and circumferential strain and strain rate were measured with STE. Segmental functional recovery was defined by improved wall-motion score on side-by-side comparison of echocardiographic images before and 9 months after revascularization and areas under the receiver operator characteristic curves were used to compare methods.

RESULTS Of the 375 segments with abnormal resting function, 154 (41%) showed functional recovery. Only circumferential resting and low-dose STE strain and low-dose longitudinal strain and SR predicted functional recovery independent of wall-motion analysis. Among different strain parameters, only TVI-based longitudinal end-systolic strain and peak systolic SR at LDD had incremental value over wall-motion analysis (areas under the receiver operator characteristic curves of 0.79, 0.79, and 0.74, respectively). STE measurements of strain and SR identified viability only in the anterior circulation, whereas TVI strain and SR accurately identified viability in both anterior and posterior circulations.

CONCLUSIONS Combination of TVI or STE methods with DbE can predict viability, with TVI strain and SR at LDD being the most accurate. TVI measures can predict viability in both anterior and posterior circulations, but STE measurements predict viability only in the anterior circulation. (J Am Coll Cardiol Img 2010;3:121–31) © 2010 by the American College of Cardiology Foundation

From the Department of Medicine, University of Queensland, Brisbane, Australia. Although the authors' research group has received research support from General Electric Medical Systems, Horten, Norway, there was no specific support for this study. Sherif Nagueh, MD served as guest editor for this paper.

Manuscript received July 21, 2009; revised manuscript received September 16, 2009, accepted September 23, 2009.

The detection of myocardial viability in patients with ischemic left ventricular (LV) dysfunction has potential therapeutic and prognostic implications (1). Dobutamine echocardiography (DbE) has comparable accuracy to other approaches for the assessment of myocardial viability (2), but involves subjective assessment of wall-thickening responses to dobutamine stimulation and is highly operator-dependent (3).

Measurement of myocardial deformation with tissue-velocity imaging (TVI) during DbE has comparable accuracy to expert wall-motion analysis for prediction of functional recovery (4). However, the wider application of Doppler strain in clinical practice has been constrained by its susceptibility to signal noise and dependence on the angle of insonation (5). Angle dependency is not a problem with 2-dimensional speckle-tracking echocardiography (STE), but this technique is dependent on image quality and operates at limited frame rate (6,7). STE-based myocardial strain has been validated against other techniques, used to measure the amplitude and timing of function at rest, and applied (with more difficulty) during stress (8–10). However, its utility in the DbE assessment of myocardial viability has not been studied. In the present study, we sought to determine the relative accuracy of TVI- and STE-based measurements of myocardial strain for the detection of myocardial viability.

ABBREVIATIONS AND ACRONYMS

AUC = area under the receiver operator characteristic curve
circS = circumferential strain
circSR = circumferential strain rate
DbE = dobutamine echocardiography
LDD = low-dose dobutamine
longS = longitudinal strain
longSR = longitudinal strain rate
LV = left ventricular
radS = radial strain
radSR = radial strain rate
ROC = receiver-operator characteristic
SR = strain rate
STE = speckle-tracking echocardiography
TVI = tissue-velocity imaging

METHODS

Study design. Fifty-five patients with ischemic heart disease and LV systolic dysfunction (ejection fraction <0.45) who were undergoing DbE for assessment of myocardial viability and who subsequently underwent myocardial revascularization were included in the study. This study involved analysis of TVI images recorded by Hanekom et al. (4) and new analysis and comparison of strain and strain rate (SR) measurements with STE. A follow-up echocardiogram was performed 9 months after revascularization to assess recovery of regional myocardial function.

Dobutamine stress echocardiography. A standard dobutamine-atropine stress protocol was performed with low-dose images at 5 and 10 μg/kg/min. Blood pressure and 12-lead electrocardiography were recorded at baseline and at the end of every stage.

IMAGE ACQUISITION. Echocardiography was performed using a standard commercial echocardiography system (Vivid Seven, General Electric Medical Systems, Milwaukee, Wisconsin) with an M3S probe. Parasternal long-axis and mid-ventricular short-axis views, as well as 3 standard apical views (4-, 2-, and 3-chamber) were acquired at rest and at each stage during dobutamine stress. Gray-scale images were obtained at a frame rate of 60 to 100 frames/s using harmonic (1.7/3.4 MHz) B-mode imaging. Separate harmonic color tissue-velocity images were also acquired with a color frame rate of 100 to 185 frames/s depending on the sector width. For each view, 3 consecutive cardiac cycles were acquired during a breath hold.

WALL-MOTION ANALYSIS. Regional wall-motion analysis was performed by 2 independent observers, blinded to the patients' clinical data, using both side-by-side digital displays and review of videotape. In each of 16 LV segments (11), wall motion was scored as 1, normokinetic; 1.5, mildly hypokinetic; 2, moderate to severely hypokinetic; 3, akinetic; or 4, dyskinetic. A dysfunctional segment was considered to be viable if there was at least a 1-grade improvement at low-dose dobutamine (LDD) with or without worsening at peak dose.

MEASUREMENT OF DEFORMATION PARAMETERS. Myocardial strain and SR with STE and TVI were measured at rest and at LDD using the same 16-segment model (EchoPAC-PC 6.0, General Electric Medical Systems, Milwaukee, Wisconsin). Gray-scale harmonic images were used for STE strain measurements and color tissue-velocity images were used for measurement of TVI strain. Only longitudinal strain (longS) and longitudinal (longSR) were measured with TVI, whereas STE measured longitudinal (apical views), radial, and circumferential (short-axis view) deformation. Radial strain (radS) and circumferential strain (circS) and radial strain rate (radSR) and circumferential strain rate (circSR) were measured only in the mid-ventricular segments because only 1 short-axis view was avail-

able. Only those segments that had baseline resting wall-motion abnormalities were included in the measurement.

Measurement of myocardial strain with STE (Fig. 1). STE strain and SR were measured in 1 cardiac cycle per view. After manual tracing of the endocardial border in end systole, a region of interest was manually adjusted to include the entire myocardial thickness. The software then tracked speckles frame-by-frame throughout the entire cardiac cycle. The automated software then generated traces depicting regional strain and SR, from which end-systolic strain and peak systolic SR were recorded.

Measurement of myocardial strain with TVI. A region of interest (12 × 6 mm) was placed in the middle of each myocardial segment and tracked manually through the cardiac cycle. In each segment, traces depicting regional longS and longSR were generated over the whole cardiac cycle, and end-systolic longS and peak systolic longSR were recorded. Segments that were poorly visualized or had insonation angle >30° were excluded from the measurements.

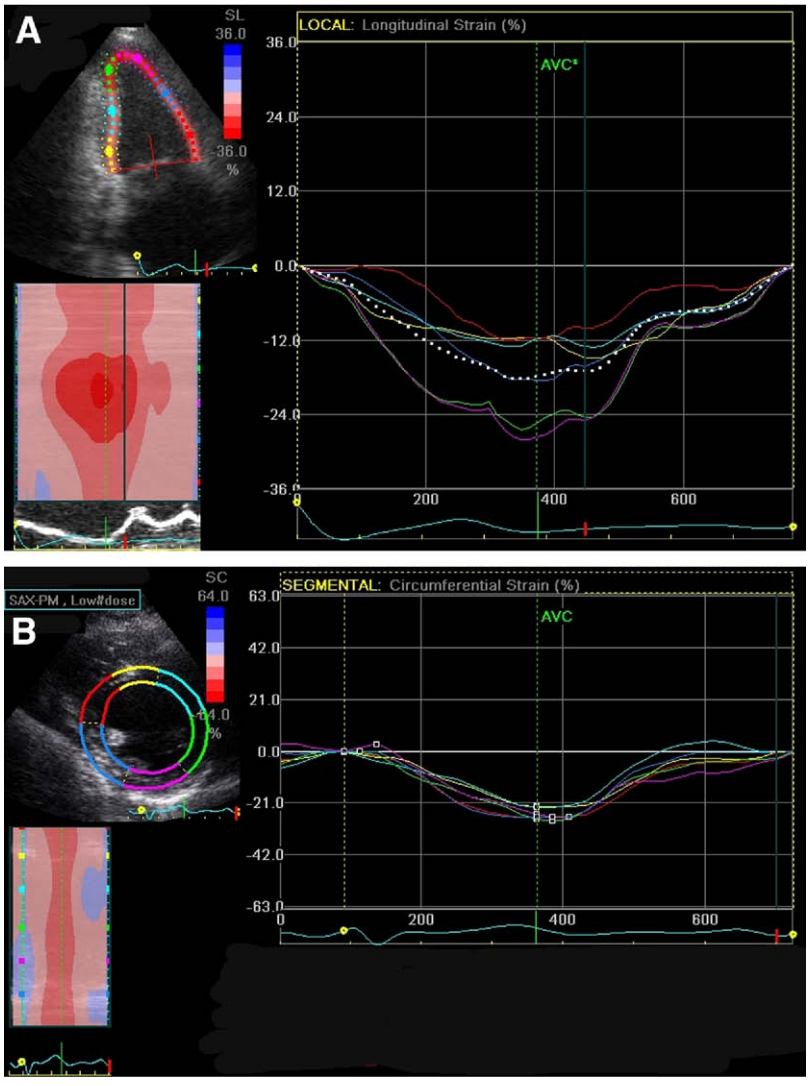

Figure 1. Measurement of Longitudinal (A) and Circumferential (B) Myocardial Strain Using Speckle-Tracking Echocardiography

Each screen illustrates the gray-scale image (respectively apical 2-chamber and mid-left ventricular short axis) from which strain is derived. Strain within each segment is coded by the color overlay of that segment, and segmental strain is plotted over time on the right of the screen. The anatomic M-mode **(lower left)** is a parametric display of strain magnitude (color coded) over time, with the segments portrayed on the y axis.

JACC: CARDIOVASCULAR IMAGING, VOL. 3, NO. 2, 2010
FEBRUARY 2010:121–31

Table 1. Clinical Characteristics of the Study Population at Baseline

Parameter	Value
Age (yrs)	66.6 ± 12.0
Male sex	46 (84%)
Hypertension (>140/90 mm Hg)	32/45 (71%)
Diabetes mellitus	21/45 (47%)
Hypercholesterolemia (total cholesterol >5 mmol/l)	10/45 (22%)
Smoking	18/45 (40%)
Family history of premature coronary artery disease	27/45 (60%)
Angina	20/45 (44%)
Heart failure	20/45 (44%)
New York Heart Association functional class	1.5 ± 0.8
Left ventricular ejection fraction (%)	35.2 ± 10.8
Beta-blockers	20/45 (44%)
Nitrates	10/45 (22%)
Calcium-channel blockers	7/45 (16%)

Values are n (%) or mean ± SD.

Table 2. Interobserver Variability of Strain Measurements

Parameter	Correlation	Mean Difference	p Value
STE-based measurements			
$LongS_{rest}$ (%)	0.75	0.73 ± 5.3	0.39
$LongSR_{rest}$ (s^{-1})	0.60	−0.13 ± 0.53	0.12
$LongS_{LDD}$ (%)	0.72	0.74 ± 5.5	0.40
$LongSR_{LDD}$ (s^{-1})	0.56	−0.01 ± 0.58	0.92
$RadS_{rest}$ (%)	0.55	−1.00 ± 15.9	0.73
$RadSR_{rest}$ (s^{-1})	0.38	−0.42 ± 1.3	0.08
$RadS_{LDD}$ (%)	0.42	2.99 ± 27.6	0.56
$RadSR_{LDD}$ (s^{-1})	0.36	−0.21 ± 0.96	0.24
$CircS_{rest}$ (%)	0.56	0.92 ± 8.3	0.55
$CircSR_{rest}$ (s^{-1})	0.42	0.05 ± 0.88	0.74
$CircS_{LDD}$ (%)	0.56	−1.39 ± 8.8	0.40
$CircSR_{LDD}$ (s^{-1})	0.50	−0.08 ± 0.81	0.58
TVI-based measurements			
$LongS_{rest}$ (%)	0.93	−1.2 ± 6.9	0.35
$LongSR_{rest}$ (s^{-1})	0.71	−0.17 ± 0.6	0.12
$LongS_{LDD}$ (%)	0.89	−0.2 ± 5.8	0.88
$LongSR_{LDD}$ (s^{-1})	0.79	−0.07 ± 1.77	0.83

CircS = circumferential strain; CircSR = circumferential strain rate; LDD = low-dose dobutamine; LongS = longitudinal strain; LongSR = longitudinal strain rate; RadS = radial strain; RadSR = radial strain rate; STE = speckle tracking echocardiography; TVI = tissue-velocity imaging.

Table 3. Myocardial Deformation Parameters at Rest and at Low-Dose Dobutamine at Baseline in the Segments That Recovered and Those That Did Not Recover After Revascularization

Variable	Functional Recovery	No Functional Recovery	p Value
STE-based measurements			
$LongS_{rest}$ (%)	−11.7 ± 6.4	−8.7 ± 7.0	<0.001
$LongSR_{rest}$ (s^{-1})	−0.89 ± 0.55	−0.70 ± 0.61	0.003
$LongS_{LDD}$ (%)	−14.6 ± 7.6	−11.4 ± 7.7	<0.001
$LongSR_{LDD}$ (s^{-1})	−1.16 ± 0.81	−1.00 ± 0.86	0.11
Δ LongS (%)	−2.8 ± 6.4	−2.3 ± 5.2	0.45
Δ LongSR (s^{-1})	−0.24 ± 0.89	−0.30 ± 0.91	0.57
$RadS_{rest}$ (%)	25.1 ± 22.8	17.0 ± 19.7	0.02
$RadSR_{rest}$ (s^{-1})	2.23 ± 1.4	2.0 ± 2.5	0.5
$RadS_{LDD}$ (%)	22.0 ± 25.3	16.1 ± 21.0	0.13
$RadSR_{LDD}$ (s^{-1})	2.32 ± 1.51	1.91 ± 1.5	0.11
Δ RadS (%)	−2.9 ± 28.9	−0.9 ± 24.6	0.7
Δ RadSR (s^{-1})	0.13 ± 1.8	−0.11 ± 2.9	0.6
$CircS_{rest}$ (%)	−12.7 ± 9.5	−7.8 ± 8.5	0.001
$CircSR_{rest}$ (s^{-1})	−1.32 ± 0.8	−1.1 ± 0.7	0.04
$CircS_{LDD}$ (%)	−13.1±8.9	−9.3 ± 7.1	0.005
$CircSR_{LDD}$ (s^{-1})	−1.46 ± 0.7	−1.12 ± 0.86	0.01
Δ CircS (%)	−0.6 ± 10.3	−1.5 ± 8.9	0.6
Δ CircSR (s^{-1})	−0.15 ± 0.9	−0.02 ± 0.9	0.4
TVI-based measurements			
$LongS_{rest}$ (%)	−8.1 ± 7.6	−5.9 ± 6.7	0.004
$LongSR_{rest}$ (s^{-1})	−0.49 ± 0.43	−0.39 ± 0.45	0.045
$LongS_{LDD}$ (%)	−14.7 ± 7.1	−7.0 ± 7.3	<0.001
$LongSR_{LDD}$ (s^{-1})	−1.05 ± 0.56	−0.52 ± 0.49	<0.001
Δ LongS (%)	−6.6 ± 7.0	−1.0 ± 5.9	<0.001
Δ LongSR (s^{-1})	−0.56 ± 0.51	−0.12 ± 0.46	<0.001

Abbreviations as in Table 2.

Revascularization and follow-up. All patients underwent percutaneous or surgical revascularization, selected according to the judgment by the treating physician. Follow-up echocardiography was performed 9 months after revascularization. Segments with resting dysfunction that were adequately revascularized were evaluated for regional recovery by 2 independent observers, blinded to patients' clinical and DbE data. Segments were deemed to have recovered if the follow-up echocardiogram revealed improvement on side-by-side comparison of resting wall motion. None of the patients had a cardiac event during follow-up.

Measurement variability. STE and TVI strain and SR were performed by 2 independent observers. To assess interobserver variability, measurements of each strain technique were repeated by an independent observer on the same echocardiographic images in 5 patients (40 myocardial segments) for longS and longSR and in 10 patients (30 myocardial segments) for radial and circumferential strain and SR.

Statistical analysis. The statistical analysis was performed using standard software (SPSS 14.0, SPSS Inc, Chicago, Illinois). Comparisons between segments showing functional recovery at follow-up and those that did not recover were performed with independent samples *t* test for continuous variables

and chi-square test for categorical variables. Receiver-operator characteristics (ROC) curves were created to assess ability of different strain parameters to predict functional recovery; the optimal cut point was based on the Youden index (12). Comparisons between ROC curves for different strain and SR parameters were made according to the method suggested by DeLong et al. (13). Because concerns have been raised about accuracy of STE strain measurements in the regions supplied by right coronary and left circumflex arteries (posterior circulation) related to image quality (9), we reanalyzed our data by different myocardial regions. Finally, multivariable logistic regression analysis was performed using functional recovery as the dependent variable to determine the independent predictive value of wall-motion analysis and various strain and SR parameters. In order to avoid problems of collinearity, this evaluation was set up in a series of separate logistic analyses for each of the deformation parameters, including wall-motion analysis and a patient-based variable (to correct for repeated measures within each patient). All values are expressed as mean ± SD or percentages. A p value of ≤0.05 was considered statistically significant.

RESULTS

Clinical characteristics of the study population. Table 1 summarizes the clinical characteristics, baseline LV ejection fraction, and ongoing medical therapy in the study population.

Wall-motion scoring and functional recovery. Only segments that had resting wall-motion abnormality that were adequately revascularized were included in the analysis. Of these 375 segments, 154 (41%) showed functional recovery at the end of follow-up. At baseline DbE, 160 segments (43%) were designated as viable on the basis of the dobutamine response. Among the segments showing functional recovery, 110 were accurately predicted by wall-motion analysis, yielding a

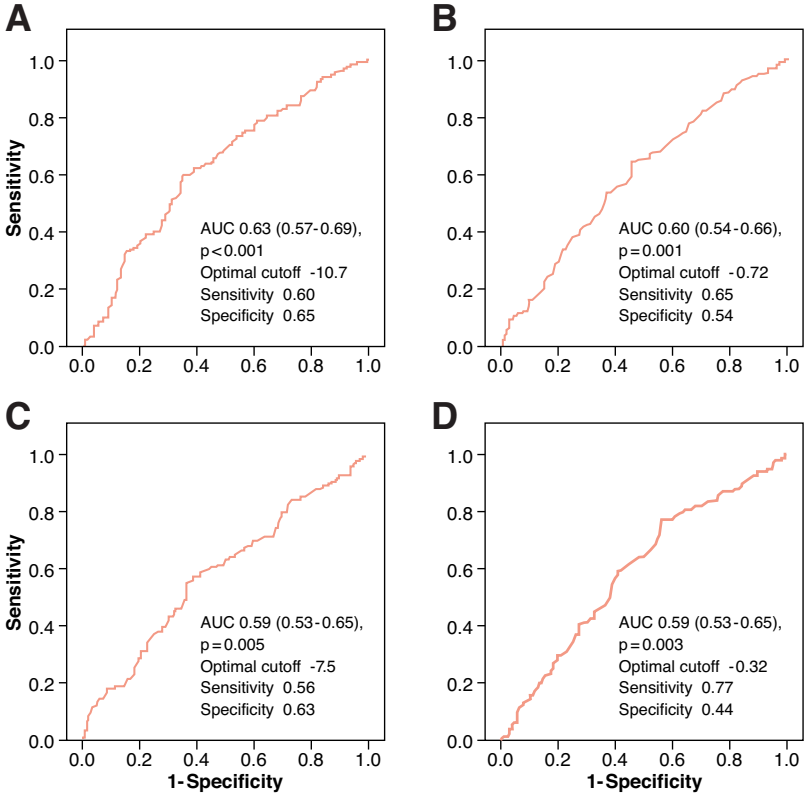

Figure 2. ROC Curves to Demonstrate Accuracy of Resting STE- and TVI-Derived Longitudinal Strain and SR for Prediction of Functional Recovery After Revascularization

(A) STE strain, **(B)** STE SR, **(C)** TVI strain, and **(D)** TVI SR. The accuracy of all parameters at rest was modest. AUC = area under the receiver operator characteristic curve; SR = strain rate; STE = speckle-tracking echocardiography; TVI = tissue-velocity imaging.

sensitivity of 71%. In contrast, wall-motion scoring correctly identified 171 of the 221 segments that did not recover after revascularization (specificity 77%, $p < 0.001$).

Feasibility and reproducibility of strain and SR measurements. We were able to perform longS and longSR measurements in 359 segments (96%) using TVI and in 344 segments (92%, $p = 0.03$) using STE. The radS, radSR, circS, and circSR measurements using STE could be performed in 97% of the available 149 segments. The interobserver variability for different strain and SR measurements with the 2 techniques is summarized in Table 2.

STE measurements and functional recovery. Table 3 summarizes various strain and SR measurements with STE in the segments with and without functional recovery. Segments showing functional recovery showed significantly higher strain in all 3 directions at rest but only longS and circS at LDD. Of SR parameters, only longSR at rest and circSR at rest and LDD showed significant difference in the 2 groups.

On ROC analysis, longS and longSR at rest and LDD, radS, and radSR at rest and circS and circSR at rest and at LDD were significant predictors of functional recovery (Figs. 2 to 5). Increments in any of these variables in response to dobutamine stimulation were not found to be predictors of functional recovery. Comparison of the ROC curves showed no significant difference with respect to their predictive accuracy for functional recovery.

TVI measurements and functional recovery. Both longS and longSR at rest and at LDD were significantly higher in segments that recovered after revascularization as compared with those that did not recover (Table 3). All strain and SR parameters predicted functional recovery (Figs. 2 and 3), but longS and longSR at LDD were stronger predictors of functional recovery than the corresponding parameters at rest (all p values

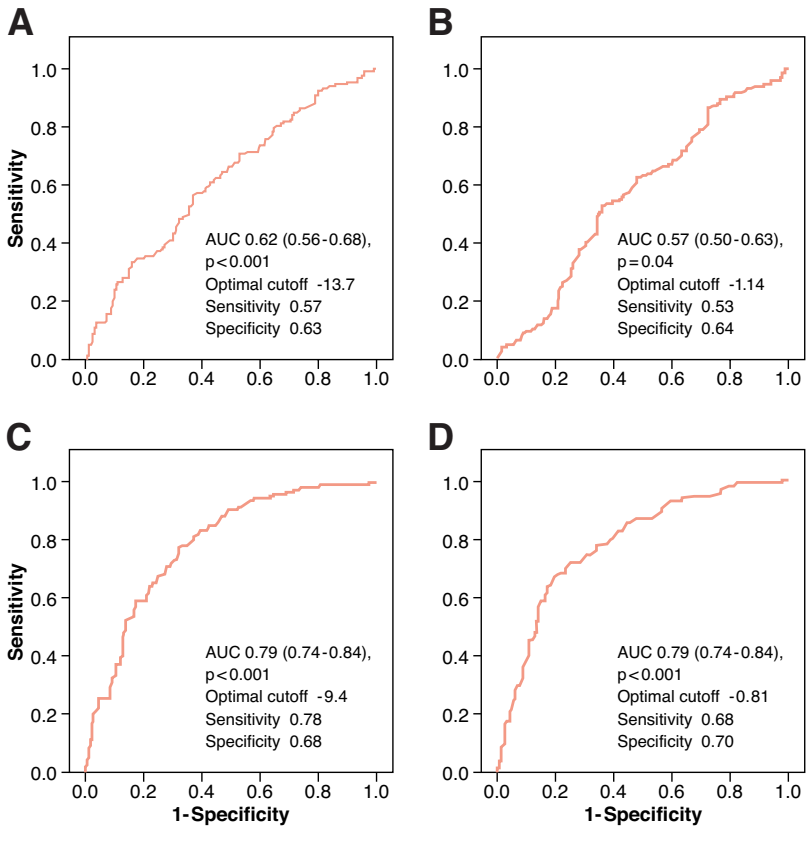

Figure 3. ROC Curves to Demonstrate Accuracy of STE- and TVI-Derived Longitudinal Strain and SR at Low-Dose Dobutamine for Prediction of Functional Recovery After Revascularization

(A) STE strain, **(B)** STE SR, **(C)** TVI strain, and **(D)** TVI SR. The accuracy of the TVI parameters was greater than that obtained using STE. Abbreviations as in Figure 2.

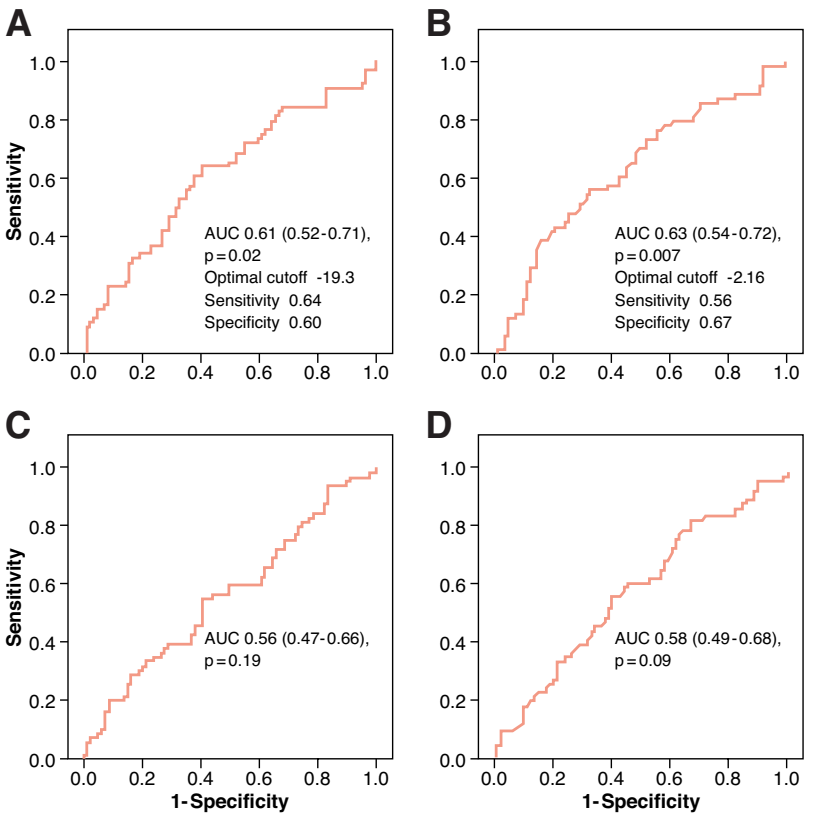

Figure 4. ROC Curves to Demonstrate Accuracy of Rest and LDD STE-Based Radial Strain and SR for Prediction of Functional Recovery After Revascularization

(A) Resting radial strain, **(B)** resting radial SR, **(C)** LDD radial strain, and **(D)** LDD radial SR. The accuracy of all parameters was modest. LDD = low-dose dobutamine; other abbreviations as in Figure 2.

<0.001). The increment in longS (area under the receiver-operator characteristic curve [AUC] 0.73 [95% confidence interval: 0.68 to 0.79], $p < 0.001$; optimal cutoff −3.0 for sensitivity and specificity 0.70) and **Δ**longSR (AUC 0.76 [95% confidence interval: 0.71 to 0.81], $p < 0.001$; optimal cutoff −0.24 for sensitivity 0.77 and specificity 0.68) with dobutamine stimulation were also good predictors of recovery.

Comparison among wall-motion analysis and STE- and TVI-based strain measurements. TVI longS and longSR at LDD (AUC 0.79 and 0.79, respectively) were the only predictors of functional recovery close to an AUC of 0.8 (the usual threshold for a "good" test). There was no significant difference in the diagnostic accuracy between these parameters and wall-motion analysis during DbE (AUC 0.74).

Because there was a significant linear relationship between corresponding strain and SR measurements, separate multivariable analyses were performed to determine whether any of the deformation measurements had incremental value over wall-motion analysis for prediction of functional recovery. Only circumferential resting and low-dose strain and TVI-based longS and longSR at LDD emerged as independent predictors of functional recovery (Table 4).

Regional differences in the predictive accuracy of strain and SR parameters. To address concerns about the influence of image quality on the accuracy of STE strain measurements, we reanalyzed our data separately for different myocardial regions. For this purpose, basal and mid-segments of posterior, lateral, and inferior walls and basal interventricular septum were designated to the posterior circulation. On ROC curve analysis, most of the STE strain and SR parameters were found to predict functional recovery in the anterior circulation. In contrast, both longS and longSR at LDD with TVI were highly significant predictors of functional recovery in both anterior and posterior circulations (Table 5).

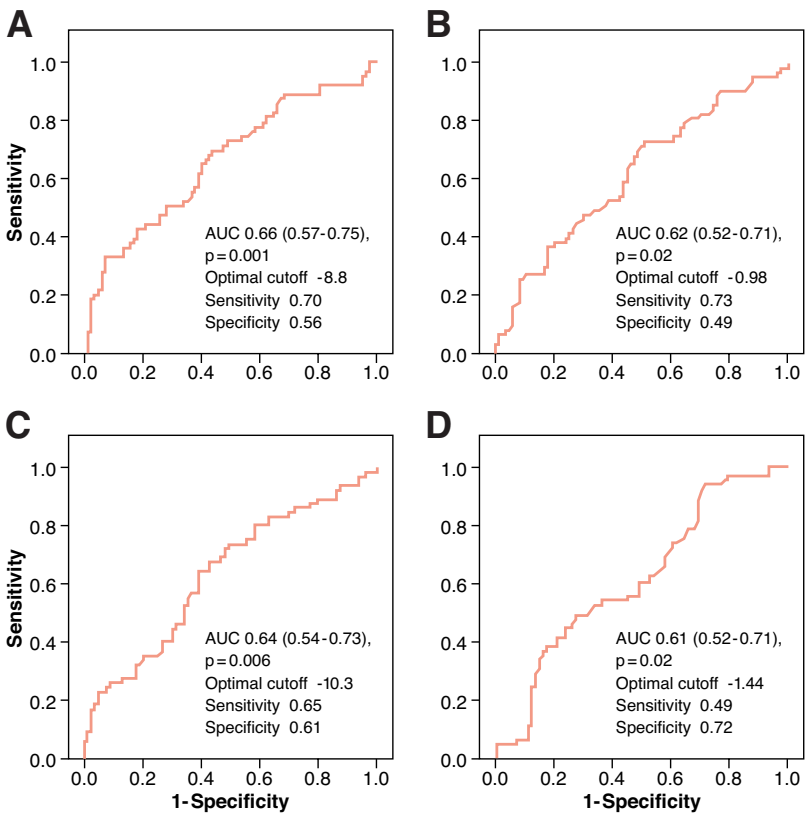

Figure 5. ROC Curves to Demonstrate Accuracy of Rest and LDD Circumferential STE-Based Strain and SR for Prediction of Functional Recovery After Revascularization

(A) Resting circumferential strain, **(B)** resting circumferential SR, **(C)** LDD circumferential strain, and **(D)** LDD circumferential SR at LDD. The accuracy of all parameters was modest. LDD = low-dose dobutamine; other abbreviations as in Figure 2.

DISCUSSION

The salient findings of the present study are as follows: 1) *longitudinal* strain and SR measured at rest and at LDD using either TVI or STE are predictors of functional recovery after revascularization; 2) STE measurements of *circumferential* strain and SR at rest and LDD and *radial* strain and SR at rest also predict functional recovery; 3) only TVI based longitudinal strain and SR at LDD have incremental value over wall-motion analysis in prediction of function recovery; and 4) STE measurements identify viability in the anterior circulation, whereas TVI strain and SR accurately identify viability in both anterior and posterior circulations.

Longitudinal deformation and prediction of functional recovery. Efforts have been made to develop quantitative measures of myocardial function that could be incorporated during DbE to enhance its accuracy and reproducibility (4,14). Although no previous study has evaluated accuracy of STE measurements of longitudinal deformation for viability testing with DbE, their correlation with the transmural extent of infarct tissue has been studied (15). In 80 patients with chronic ischemic LV dysfunction, Chan et al. (15) found no difference in resting STE longS and longSR between subendocardial and transmural infarct segments. However, at LDD, both longS and longSR were significantly lower in segments with transmural compared with those with subendocardial infarcts (15). Even resting longitudinal TVI strain may be significantly impaired in transmural infarct segments (16).

In the present study, although STE longS and longSR were significant predictors of functional recovery, their accuracy was only modest and much lower than the TVI-based longS and longSR at LDD. Moreover, only TVI measurements and none of the STE measurements were found to have incremental value over wall-motion analysis. These

Table 4. Multivariate Logistic Regression Analysis to Assess Independent Predictive Accuracy of Different Myocardial Strain and Strain Rate Measurements for Functional Recovery After Revascularization

	Deformation Parameter		Wall-Motion Analysis	
Variable	OR (95% CI)	p Value	OR (95% CI)	p Value
Strain				
STE $LongS_{rest}$	0.98 (0.94–1.01)	0.19	6.9 (4.1–11.3)	<0.0001
STE $LongS_{LDD}$	0.99 (0.96–1.03)	0.73	7.4 (4.3–12.9)	<0.0001
STE $RadS_{rest}$	1.00 (0.99–1.03)	0.31	7.0 (3.3–15.1)	<0.0001
STE $RadS_{LDD}$	1.03 (0.99–1.02)	0.70	7.5 (3.5–16.1)	<0.0001
STE $CircS_{rest}$	0.95 (0.91–0.99)	0.01	7.1 (3.3–15.3)	<0.0001
STE $CircS_{LDD}$	0.95 (0.91–0.99)	0.04	7.2 (3.4–15.4)	<0.0001
TVI $LongS_{rest}$	0.99 (0.96–1.03)	0.60	8.7 (5.3–14.4)	<0.0001
TVI $LongS_{LDD}$	0.88 (0.85–0.92)	<0.0001	5.4 (3.2–9.1)	<0.0001
Strain rate				
STE $LongSR_{rest}$	0.84 (0.54–1.30)	0.43	7.1 (4.3–11.6)	<0.0001
STE $LongSR_{LDD}$	0.98 (0.72–1.34)	0.90	7.4 (4.4–12.5)	<0.0001
STE $RadSR_{rest}$	0.96 (0.82–1.13)	0.64	7.9 (3.7–17.0)	<0.0001
STE $RadSR_{LDD}$	1.19 (0.93–1.52)	0.17	7.7 (3.7–16.4)	<0.0001
STE $CircSR_{rest}$	0.73 (0.43–1.24)	0.24	7.1 (3.3–15.0)	<0.0001
STE $CircSR_{LDD}$	0.67 (0.41–1.09)	0.11	7.2 (3.4–15.3)	<0.0001
TVI $LongSR_{rest}$	1.09 (0.62–1.91)	0.76	9.1 (5.5–15.1)	<0.0001
TVI $LongSR_{LDD}$	0.20 (0.11–0.37)	<0.0001	5.6 (3.3–9.4)	<0.0001

CI = confidence interval; OR = odds ratio; other abbreviations as in Table 2.

limitations of STE at stress may relate to its dependence on gray-scale image quality or the low frame rate of this technique.

Radial and circumferential deformation and prediction of functional recovery. The LV wall is composed of multiple layers of myocardial fibers, responsible

Table 5. Receiver-Operator Characteristics Curve Analysis to Assess Accuracy of Various Myocardial Deformation Parameters for Prediction of Functional Recovery in Different Myocardial Regions

	Anterior Circulation		Posterior Circulation	
Variable	Area Under the Curve (95% CI)	p Value	Area Under the Curve (95% CI)	p Value
STE-based measurements				
$LongS_{rest}$	0.68 (0.60–0.75)	<0.001	0.59 (0.50–0.68)	NS
$LongSR_{rest}$	0.63 (0.54–0.71)	0.003	0.59 (0.50–0.68)	0.045
$LongS_{LDD}$	0.65 (0.56–0.73)	0.002	0.60 (0.51–0.69)	0.04
$LongSR_{LDD}$	0.60 (0.50–0.69)	0.043	0.56 (0.48–0.65)	NS
$RadS_{rest}$	0.63 (0.50–0.76)	0.07	0.61 (0.48–0.74)	NS
$RadSR_{rest}$	0.65 (0.52–0.78)	0.03	0.63 (0.50–0.77)	0.07
$RadS_{LDD}$	0.60 (0.47–0.73)	NS	0.53 (0.40–0.67)	NS
$RadSR_{LDD}$	0.59 (0.45–0.72)	NS	0.61 (0.47–0.74)	NS
$CircS_{rest}$	0.69 (0.57–0.82)	0.005	0.62 (0.49–0.75)	NS
$CircSR_{rest}$	0.63 (0.50–0.76)	0.06	0.62 (0.49–0.75)	NS
$CircS_{LDD}$	0.69 (0.56–0.82)	0.006	0.59 (0.46–0.72)	NS
$CircSR_{LDD}$	0.67 (0.54–0.80)	0.02	0.56 (0.43–0.70)	NS
TVI-based measurements				
$LongS_{rest}$	0.66 (0.58–0.74)	<0.001	0.51 (0.42–0.59)	NS
$LongSR_{rest}$	0.66 (0.58–0.74)	<0.001	0.52 (0.43–0.60)	NS
$LongS_{LDD}$	0.83 (0.77–0.89)	<0.001	0.75 (0.68–0.83)	<0.001
$LongSR_{LDD}$	0.84 (0.78–0.89)	<0.001	0.75 (0.67–0.82)	<0.001

CI = confidence interval; NS = not significant; other abbreviations as in Table 2.

for shortening in different directions. Whereas longitudinal contraction is primarily a property of subendocardial fibers, contraction in radial and circumferential directions is brought about predominantly by fibers in the outer layers (17–19). Consequently, short-axis function is likely to be less affected in subendocardial than transmural infarction (15,20) and has been proposed as a marker of myocardial viability (21).

Unlike the previous studies, we showed that the augmentation in short-axis contractile function in response to low-dose dobutamine showed circS but not radS to remain a predictor of viability. This finding may reflect cross-fiber shortening, whereby passive radial thickening of segments with nontransmural infarction is generated by viable epicardial fibers (18). The finding that resting circS was the most accurate STE-strain measurement is congruent with circS offering the greatest contrast between subendocardial and transmural infarcts (14).

Limitations. The radS and circS were not measured in the apical and basal segments, and this may explain why only circS was found to have independent predictive value. The lack of apical measurements could have been particularly important, as STE performed much better in the anterior than the posterior circulation.

This is a study of relatively small sample size using a wall-motion end point, which restricts the findings to this center's experience. The results may be different with a different patient sample with different degrees of transmural versus subendocardial scar, different revascularization outcome success, and other different confounding variables.

CONCLUSIONS

Strain and SR measurement with both TVI and STE are feasible during DbE and can predict recovery of regional contractile function after revascularization. However, TVI strain and SR measurements at low-dose dobutamine are more accurate for this purpose and can predict viability in both anterior and posterior circulations. In contrast, STE measurements appear to be most effective in the anterior circulation.

Reprint requests and correspondence: Dr. Thomas H. Marwick, University of Queensland Department of Medicine, Princess Alexandra Hospital, Ipswich Road, Brisbane, Qld 4102, Australia. *E-mail: t.marwick@uq.edu.au.*

REFERENCES

1. Allman KC, Shaw LJ, Hachamovitch R, Udelson JE. Myocardial viability testing and impact of revascularization on prognosis in patients with coronary artery disease and left ventricular dysfunction: a meta-analysis. J Am Coll Cardiol 2002;39:1151–8.
2. Bax JJ, Wijns W, Cornel JH, Visser FC, Boersma E, Fioretti PM. Accuracy of currently available techniques for prediction of functional recovery after revascularization in patients with left ventricular dysfunction due to chronic coronary artery disease: comparison of pooled data. J Am Coll Cardiol 1997;30:1451–60.
3. Picano E, Lattanzi F, Orlandini A, Marini C, L'Abbate A. Stress echocardiography and the human factor: the importance of being expert. J Am Coll Cardiol 1991;17:666–9.
4. Hanekom L, Jenkins C, Jeffries L, et al. Incremental value of strain rate analysis as an adjunct to wall-motion scoring for assessment of myocardial viability by dobutamine echocardiography: a follow-up study after revascularization. Circulation 2005;112:3892–900.
5. Urheim S, Edvardsen T, Torp H, Angelsen B, Smiseth OA. Myocardial strain by Doppler echocardiography. Validation of a new method to quantify regional myocardial function. Circulation 2000;102:1158–64.
6. Leitman M, Lysyansky P, Sidenko S, et al. Two-dimensional strain—a novel software for real-time quantitative echocardiographic assessment of myocardial function. J Am Soc Echocardiogr 2004;17:1021–9.
7. Langeland S, D'Hooge J, Wouters PF, et al. Experimental validation of a new ultrasound method for the simultaneous assessment of radial and longitudinal myocardial deformation independent of insonation angle. Circulation 2005;112:2157–62.
8. Becker M, Bilke E, Kuhl H, et al. Analysis of myocardial deformation based on pixel tracking in two dimensional echocardiographic images enables quantitative assessment of regional left ventricular function. Heart 2006;92:1102–8.
9. Hanekom L, Cho GY, Leano R, Jeffriess L, Marwick TH. Comparison of two-dimensional speckle and tissue Doppler strain measurement during dobutamine stress echocardiography: an angiographic correlation. Eur Heart J 2007;28:1765–72.
10. Cho GY, Chan J, Leano R, Strudwick M, Marwick TH. Comparison of two-dimensional speckle and tissue velocity based strain and validation with harmonic phase magnetic resonance imaging. Am J Cardiol 2006;97:1661–6.
11. Armstrong WF, Pellikka PA, Ryan T, Crouse L, Zoghbi WA. Stress echocardiography: recommendations for performance and interpretation of stress echocardiography. Stress Echocardiography Task Force of the Nomenclature and Standards Committee of the American Society of Echocardiography. J Am Soc Echocardiogr 1998;11:97–104.
12. Youden WJ. Index for rating diagnostic tests. Cancer 1950;3:32–5.
13. DeLong ER, DeLong DM, Clarke-Pearson DL. Comparing the areas under two or more correlated receiver operating characteristic curves: a nonparametric approach. Biometrics 1988;44:837–45.
14. Hoffmann R, Altiok E, Nowak B, et al. Strain rate measurement by Doppler echocardiography allows improved assessment of myocardial viability inpatients with depressed left ventricular function. J Am Coll Cardiol 2002;39:443–9.

15. Chan J, Hanekom L, Wong C, Leano R, Cho GY, Marwick TH. Differentiation of subendocardial and transmural infarction using two-dimensional strain rate imaging to assess short-axis and long-axis myocardial function. J Am Coll Cardiol 2006;48:2026–33.
16. Zhang Y, Chan AK, Yu CM, et al. Strain rate imaging differentiates transmural from non-transmural myocardial infarction: a validation study using delayed-enhancement magnetic resonance imaging. J Am Coll Cardiol 2005;46:864–71.
17. Torrent-Guasp F, Buckberg GD, Clemente C, Cox JL, Coghlan HC, Gharib M. The structure and function of the helical heart and its buttress wrapping. I. The normal macroscopic structure of the heart. Semin Thorac Cardiovasc Surg 2001;13:301–19.
18. Rademakers FE, Rogers WJ, Guier WH, et al. Relation of regional cross-fiber shortening to wall thickening in the intact heart. Three-dimensional strain analysis by NMR tagging. Circulation 1994;89:1174–82.
19. Clark NR, Reichek N, Bergey P, et al. Circumferential myocardial shortening in the normal human left ventricle. Assessment by magnetic resonance imaging using spatial modulation of magnetization. Circulation 1991;84:67–74.
20. Becker M, Hoffmann R, Kuhl HP, et al. Analysis of myocardial deformation based on ultrasonic pixel tracking to determine transmurality in chronic myocardial infarction. Eur Heart J 2006;27:2560–6.
21. Becker M, Lenzen A, Ocklenburg C, et al. Myocardial deformation imaging based on ultrasonic pixel tracking to identify reversible myocardial dysfunction. J Am Coll Cardiol 2008; 51:1473–81.

Key Words: tissue Doppler imaging ■ regional myocardial function ■ heart failure.